ISSN 0010-5082, Combustion, Explosion, and Shock Waves, 2019, Vol. 55, No. 5, pp. 580–588. © Pleiades Publishing, Ltd., 2019.
Original Russian Text © T.A. Khmel.

Modeling of Cellular Detonation in Gas Suspensions of Submicron and Nano-Sized Aluminum Particles

T. A. Khmel[a]

UDC 532.529.5+541.126

Published in *Fizika Goreniya i Vzryva*, Vol. 55, No. 5, pp. 73–82, September–October, 2019.
Original article submitted May 10, 2018; revision submitted June 5, 2018; accepted for publication July 11, 2018.

Abstract: Cellular detonation in monodisperse suspensions of submicron and nano-sized aluminum particles is numerically simulated. Approaches of mechanics of heterogeneous media are applied. The transition from the continuum to free-molecular regime of the flow around the particles is taken into account in the processes of interphase interaction. Particle combustion is described within the framework of the semi-empirical model developed previously. Results calculated for two-dimensional flows in a plane channel for suspensions of aluminum particles with the particle size ranging from 1 μm to 100 nm are presented. The regular structure of cellular detonation is found to transform to an irregular structure as the particle size decreases. An increase in the peak pressure and enlargement of the detonation cell are also noted, which is attributed to enhancement of the activation energy of reduced kinetics caused by the transition to the kinetic regime of combustion of aluminum particles.

Keywords: gas suspension, micro- and nano-disperse aluminum powders, cellular detonation, numerical simulation.

DOI: 10.1134/S0010508219050095

INTRODUCTION

Various issues of combustion of nanodisperse aluminum powders, including that in the detonation regime, attract much attention owing to significant prospects of their applications. Detonation phenomena in gas suspensions of micro-sized spherical or flake-shaped aluminum particles were intensely studied experimentally, and the possibility of detonation propagation in the spin mode or in the form of cellular detonation was established [1–4]. Theoretical models of aluminum detonation in air, products of detonation of gas media, and oxygen were developed in [5–9].

Numerical simulations of cellular detonation for suspensions of spherical microparticles were performed in [10–12]. The detonation cell size as a function of the microparticle diameter was determined in [11, 12]. For oxygen mixtures, the data of these investigations turned out to be very close to each other, though the calculations were performed with the use of different models of particle combustion kinetics.

The interest to nanodisperse media, in particular, aluminum nanoparticles, has recently revived. A large number of new experimental data on ignition and combustion of submicron and nano-sized aluminum particles have been obtained. A detailed review of these results can be found in [13], where theoretical approaches to the description of heat transfer and motion of nanoparticles in the flow were also discussed.

Unfortunately, there are few investigations of detonation of submicron and nano-sizes aluminum particles. The study of Zhang et al. [4] can be noted, who observed spin detonation in an air suspension of 100-nm spherical particles and 2-μm particles. They analyzed both the common properties (similar detonation velocity and spin pitch) and specific features of detonation of the suspension of nanoparticles, e.g., significantly higher amplitudes of fluctuations of flow parameters behind the front.

[a] Khristianovich Institute of Theoretical and Applied Mechanics, Siberian Branch, Russian Academy of Sciences, Novosibirsk, 630090 Russia; khmel@itam.nsc.ru.

Mathematical modeling of detonation in suspensions of aluminum nanoparticles was performed for the first time in [14]. A semi-empirical model of detonation was developed and verified against available experimental data on ignition, combustion, and detonation of aluminum nanoparticles. The description of thermal and velocity relaxation of the phases took into account the effects of free-molecular interaction of particles with the gas, which was expressed as the dependence of the characteristic relaxation time on the Knudsen number. The analysis of the structure of plane waves of overdriven, normal, and weak detonation demonstrated that the burning time of the suspension of nanoparticles was significantly (by orders of magnitude for 100-nm particles) longer than the time of thermal and velocity relaxation, i.e., in fact, the combustion process proceeded in an equilibrium mixture in terms of velocity and temperature. Moreover, a specific feature of detonation combustion is a strong dependence of the combustion zone length on the shock wave (SW) amplitude. This is caused by the transition from the diffusion-limited regime of combustion typical for micro-sized particles [7] to the kinetic regime characterized by an appreciably higher activation energy of the combustion reaction [13]. Because of these properties, suspensions of aluminum nanoparticles are close to gases; for this reason, it is of interest how this fact will affect the cellular detonation characteristics. The goal of the present study is to investigate cellular detonation in gas suspensions of aluminum nanoparticles on the basis of numerical simulation of two-dimensional flows.

1. PHYSICOMATHEMATICAL MODEL OF DETONATION OF THE SUSPENSION OF ALUMINUM NANOPARTICLES

The governing equations describe the mass, momentum, and energy conservation laws for each phase and each species. The system is closed by the equations of state and relations for mass transfer between the species (evaporation, condensation, and combustion), exchange of momentum (drag forces), and heat transfer between the gas and particles. Two-dimensional flows in the Cartesian coordinate system are described by the following equations [11]:

$$\frac{\partial \rho_i}{\partial t} + \frac{\partial \rho_i u_i}{\partial x} + \frac{\partial \rho_i v_i}{\partial y} = (-1)^{i-1} J,$$

$$\frac{\partial \rho_i u_i}{\partial t} + \frac{\partial [\rho_i u_i^2 + (2-i)p]}{\partial x} + \frac{\partial \rho_i u_i v_i}{\partial y} = (-1)^{i-1}(-f_x + J u_2),$$

$$\frac{\partial \rho_i v_i}{\partial t} + \frac{\partial (\rho_i u_i v_i)}{\partial x} + \frac{\partial [\rho_i v_i^2 + (2-i)p]}{\partial y} = (-1)^{i-1}(-f_y + J v_2),$$

$$\frac{\partial \rho_i E_i}{\partial t} + \frac{\partial [\rho_i u_i (E_i + (2-i)p/\rho_1)]}{\partial x} + \frac{\partial [\rho_i v_i (E_i + (2-i)p/\rho_1)]}{\partial y} = (-1)^{i-1}(-q - f_x u_2 - f_y v_2 + J E_2), \tag{1}$$

$$f_2 = \frac{\rho_2}{\tau_u}(u_1 - u_2), \quad q_2 = \frac{\rho_2 c_{v,2}}{\tau_T}(T_1 - T_2),$$

$$J_2 = \frac{\rho_2}{\tau_\xi}(\xi - \xi_k), \; p = \rho_1 R T_1, \; E_1 = \frac{u_1^2}{2} + c_{v,1} T_1,$$

$$E_2 = \frac{u_2^2}{2} + c_{v,2} T_2 + Q, \quad e_2 = c_{v,2} T_2 + Q.$$

Here the subscripts 1 and 2 refer to the gas and particles, respectively, p is the pressure, $\rho_i = m_i \rho_{ii}$, u_i, E_i, T_i, $c_{v,i}$, and m_i are the mean density, velocity, total energy per unit mass, temperature, specific heat, and volume concentration of the species, respectively, ρ_{ii} is the true density, R is the reduced gas constant, and Q is the thermal effect of the particle combustion reaction within the framework of reduced kinetics. Interphase interaction is expressed by the parameters J_2 (mass transfer), f_2 (force of interphase interaction), and q_2 (heat transfer between the phases). It should be noted that two-dimensional flows are calculated by using a simplified approach justified in [15], where the heat release of the chemical reaction is determined with allowance for the melting and evaporation heats without identifying these processes as individual stages, similar to [11].

The processes of velocity relaxation and heat transfer in gas suspensions are characterized by the transition from the continuum to free-molecular regime of particle interaction with gas molecules. The allowance for free-molecular effects in the model [14] is based on available reported data, in particular, in [13]. The drag force of particles in a gas flow in the case where the particle size is comparable with the mean free path of gas molecules is determined with due allowance for the Cunningham correction factor [13]:

$$\tau_u = 4 d \rho_{22} C_{\mathrm{C}} / 3 c_D \rho_{11} |u_1 - u_2|, \tag{2}$$

$$C_{\mathrm{C}} = 1 + 2\mathrm{Kn}[1.257 + 0.4 \exp(-1.1/2\mathrm{Kn})].$$

Here $\mathrm{Kn} = RT_1/(\sqrt{2}\pi d_g^2 N_{\mathrm{A}} p d_2)$ is the Knudsen number, d_2 and ρ_{22} are the diameter and inherent density of particles, d_g and m_g are the size and mass of the ambient gas molecules, and N_{A} is the Avogadro number. The drag coefficient c_D is determined in the same manner as that for microparticles, with allowance for the

supersonic flow in the detonation structure (see [11]), by the formula

$$c_D(\mathrm{Re}, \mathrm{M}_{12}) = \left[1 + \exp\Big(-\frac{0.43}{\mathrm{M}_{12}^{4.67}}\Big)\right] \times \left(0.38 + \frac{24}{\mathrm{Re}} + \frac{4}{\sqrt{\mathrm{Re}}}\right), \quad (3)$$

$$\mathrm{Re} = \frac{\rho_{11} d|u_1 - u_2|}{\mu_1}, \quad \mathrm{M}_{12} = \frac{|u_1 - u_2|\sqrt{\rho_{11}}}{\sqrt{\gamma_1 p}}.$$

where M is the Mach number, μ_1 is the dynamic viscosity of the gas, and γ_1 is the ratio of specific heats.

The heat transfer between the gas and submicron particles and also nanoparticles is determined in accordance with the change in the flow around the particles from the continuum regime at $\mathrm{Kn} < 0.01$ to the free-molecular regime at $\mathrm{Kn} > 10$ [13]. The presentations for the characteristic times of thermal relaxation in these regimes have different forms:

$$\tau_T^{\mathrm{cont}} = \frac{d^2 \rho_{22} c_{v2}}{6\lambda_1 \mathrm{Nu}}, \quad \mathrm{Nu} = 2 + 0.6\mathrm{Re}^{1/2}\mathrm{Pr}^{1/3},$$

$$\tau_T^{fm} = \frac{d\rho_{22} c_{v2}}{6\alpha p}\sqrt{\frac{8\pi m_g T_1}{k_{\mathrm{B}}}}\left(\frac{\gamma_1 - 1}{\gamma_1 + 1}\right). \quad (4)$$

Here c_{v2} is the specific heat of particles, Nu and Pr are the Nusselt and Prandtl numbers (it is usually assumed that $\mathrm{Pr} = 0.7$), λ_1 is the thermal conductivity of the gas, k_{B} is the Boltzmann constant, and α is the accommodation coefficient. In the range of the particle sizes from 10 nm to 1 μm, the Knudsen number changes approximately from 10^{-2} to 10, and the transitional flow regime is observed. The characteristic time of heat transfer in this region is determined by means of logarithmic interpolation [14]:

$$\tau_T^{tr} = [(\log \mathrm{Kn} + 2)\tau_T^{fm} + (1 - \log \mathrm{Kn})\tau_T^{\mathrm{cont}}]/3. \quad (5)$$

The description of ignition and combustion of aluminum nanoparticles under detonation conditions can be found in [14]; it is based on the analysis of available empirical data. According to the experimental results [13], ignition of nanoparticles, even under static conditions, occurs at temperatures close to the aluminum melting point. Following [14], we use the temperature criterion of ignition $T_{\mathrm{ign}} = T_{\mathrm{melt}} = 930$ K for conditions behind the shock waves.

Particle combustion is described within the framework of reduced kinetics with constants determined on the basis of available experimental data on the dependence of the particle burning time on the particle diameter, and also on the pressure, temperature, and fraction of the oxidizer in the ambient gas [14]. For conditions of the oxidizer excess (including the stoichiometric composition), the formula is

$$\tau_\xi = \tau_0 (d/d_0)^{0.3} \exp(E_a/RT_1)(p/p_*)^{-m}. \quad (6)$$

The values of the constants for the nanometer range of particles $50 \leqslant d_0 \leqslant 135$ nm were determined in [14]: $d_0 = 80$ nm, $p_* = 8$ atm, $E_a = E_{an} = 60$ kJ/mol, $m = 0.5$, and $\tau_0 = 0.25$ μm. For micron-sized particles, a similar formula with $m = 0$, $E_a = E_{am} = 32$ kJ/mol, $d_0 = 3.5$ μm, and $\tau_0 = 0.294$ μs was derived in [16]. For the submicron range of particle sizes $135\ \mathrm{nm} \leqslant d_0 \leqslant 1$ μm, the following interpolation dependence for m and E_a is chosen:

$$m = -0.25 \ln(d/d_1), \quad (7)$$

$$E_a = E_{am}[1 + 0.5 \ln(d/d_1)] - 0.5 E_{an} \ln(d/d_1).$$

At $\tau_0 = 0.2$ μs, $p_* = 17$ atm, and $d_1 = 1$ μm, this formula ensures smooth matching of the characteristics of combustion of micro- and nanoparticles.

2. FORMULATION OF THE PROBLEM AND METHOD OF ITS SOLUTION

The initial-boundary-value problem is formulated as initiation of detonation by a strong SW entering a gas suspension cloud filling the entire width of a plane channel with a certain perturbation of density at the edge [11]. The previously tested Harten TVD scheme was used in the computations for the gas, and the Jentry–Martin–Daly scheme was applied for the particles [17]. The grid step was determined in accordance with the relaxation region scales and depended on the particle size. Test computations were performed with variation of the grid step and with free-molecular effects (Cunningham correction factor and Knudsen number in heat transfer processes) being taken into account and ignored. Figure 1 shows the fields of the maximum pressure obtained on different grids for $d = 300$ nm, $E_a = E_{an}$, $m = 0.5$, and $\tau_0 = 0.5$ μs with free-molecular effects being ignored (Figs. 1a and 1b) and taken into account (Fig. 1c). It should be noted that all pictures in Figs. 1–5 are shown in one shadow scale. As is seen from Fig. 1, despite grid step variation, the results coincide both in terms of the position and shape of the leading front and in terms of the steady-state patterns of the arrangement and motion of transverse waves. As for the plane wave structure [14], the effects of the free-molecular flow and heat transfer play a minor role for gas suspensions with the particle size greater than 300 nm.

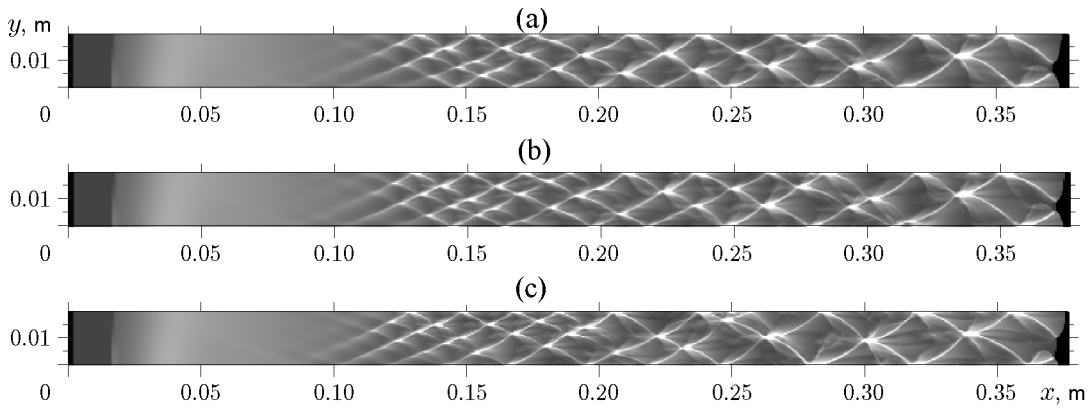

Fig. 1. Results of test calculations for $d = 300$ nm with free-molecular effects being ignored (a and b) and taken into account (c): $\Delta x = \Delta y = 0.0001$ (a), 0.000075 (b), and 0.00005 m (c).

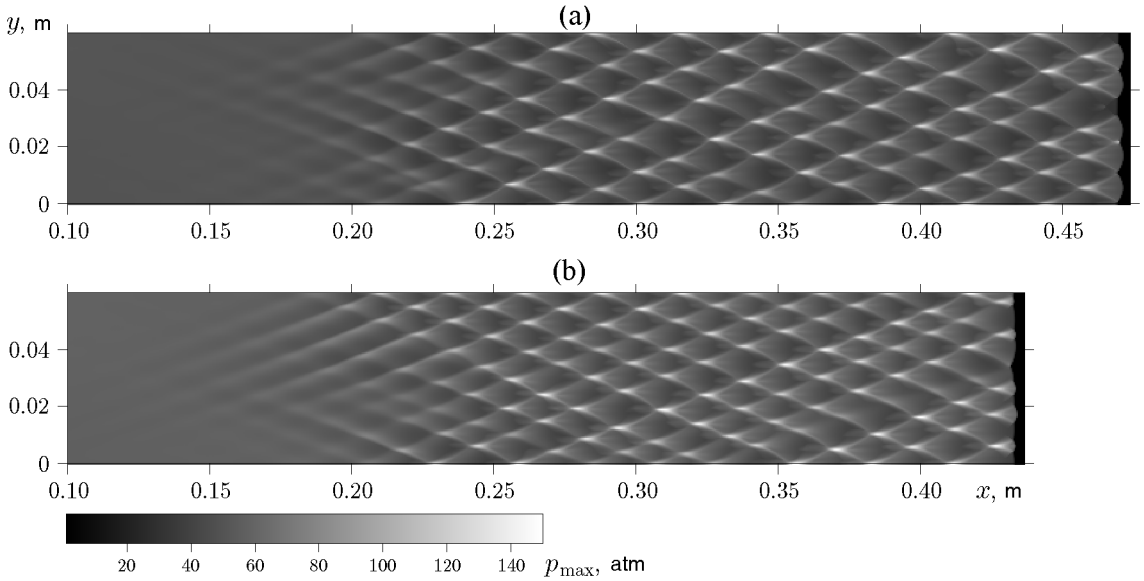

Fig. 2. Cellular detonation in gas suspensions of aluminum particles 1 μm in size for $\xi_0 = 0.4$ (a) and 0.55 (b).

3. FORMATION OF CELLULAR DETONATION IN GAS SUSPENSIONS OF MICRON AND SUBMICRON PARTICLES

A detailed study of cellular detonation in gas suspensions of aluminum microparticles was performed in [11], where the main characteristics and characteristic sizes of detonation cells for stoichiometric suspensions in oxygen were determined. A power-law dependence of the cell size on the particle diameter with the power-law index of 1.6 was derived. Similar dependences of the cell size on the particle diameter for air suspensions of aluminum particles were obtained in [12, 18], where the power-law index was found to be 1.4, which was close to that obtained in [11]. In [18], detonation modeling was performed within the framework of the kinetics [7] based on the description of particle combustion in the diffusion-limited regime. The hybrid kinetic model used in [12] included the description of low-temperature oxidation with the use of an Arrhenius-type equation in addition to the diffusion-limited combustion reaction. The comparison [12] showed that the detonation cell sizes determined with the use of both models are almost identical. It should be noted, however, that the particle burning time as a function of the particle diameter was determined both in [11] and in [12, 18] as $\tau \sim d^2$, which contradicts the latest data on combustion of fine aluminum particles reported in [13], which

testify to the existence of the transitional regime of combustion of fine micron and submicron particles from the diffusion-limited to the kinetic mode. The properties of the kinetic regime of combustion were partly taken into account in [11, 12] in the Arrhenius reaction of reduced kinetics.

In the present work, the calculations of suspensions of micron particles with diameters smaller than 3.5 μm were performed with the use of a refined model of detonation combustion of aluminum (6). In the preexponent of the Arrhenius reaction, the power-law index in the dependence of the characteristic burning time on the particle diameter was taken to be 0.3 [13]. For submicron particles with diameters smaller than 1 μm, conditions of the transitional regime were applied, and the activation energy E_a and the power-law index m in the dependence of the burning time on pressure were determined by formula (7).

Figure 2 shows some examples of the computations of cellular detonation of particles 1 μm in size for a lean mixture (in the case with oxidizer excess) and for a stoichiometric mixture. It can be noted that reduction of the initial concentration of particles exerts practically no effect on the cellular detonation characteristics: peak pressure and cell size. The mean velocity of front propagation is 1.68 km/s for $\xi_0 = 0.4$ and 1.57 km/s for $\xi_0 = 0.55$, which is slightly smaller than that predicted by the Chapman–Jouguet theory and thermodynamic computations [18] (1.7 and 1.6 km/s).

The characteristics of cellular detonation with the particle size of 1 μm are similar to those described in [11], except for a slightly greater size of the regular cell than that predicted within the framework of the kinetics with a quadratic dependence of the burning time on the particle diameter. As in [11], the peak pressures in collisions of triple points of cellular detonation are approximately 150 atm, which is almost thrice higher than the pressure at the chemical spike point of the Chapman–Jouguet waves. The trajectories of the triple points are close to straight lines. In micron-sized suspensions, a significant portion of the combustion period corresponds to the conditions of velocity and temperature equilibrium of the phases [8, 11], which is a smoothing factor of the formation of the pressure profile behind the front of the leading shock wave. For this reason, the footprints of the triple points becomes smeared as in [11] (see Fig. 2). A similar character of the trajectories and an even higher degree of their smearing with line doubling (because of the nonmonotonic behavior of the parameters in the region of velocity, thermal, and chemical relaxation) were also calculated in [12, 18] for cellular detonation of larger particles (8.6 and 13.5 μm).

Cellular detonation patterns for 600-nm particles (stoichiometric composition) are presented in Fig. 3. The peak pressure is significantly higher here: 220 atm. It can be also noted that the trajectories of the triple points are somewhat less smeared here, which makes the cellular detonation patterns approach similar patterns in gases.

A possible explanation can be formulated as follows: with a transition to the submicron range of the particle sizes, combustion is less affected by relaxation processes. The characteristic time of velocity and thermal relaxation decreases in proportion to d^α, where $1.5 < \alpha < 2$, and the burning time decreases in proportion to $d^{0.3}$ according to the data reported in [13]. Thus, propagation of detonation in submicron and nano-sized aluminum particles is characterized by combustion under the conditions of velocity and thermal equilibrium of the phases, which makes the cellular detonation characteristics approach those of detonation in gas mixtures.

The second factor responsible for the increase in the peak pressure is the change in the kinetics of combustion of aluminum particles with the transition from the diffusion-limited to kinetic regime [13]. This is most clearly visible in computations of detonation of gas suspensions of particles smaller than 500 nm.

4. SPECIFIC FEATURES OF CELLULAR DETONATION IN GAS SUSPENSIONS OF NANO-SIZED PARTICLES

The results of simulations of cellular detonation of suspensions of particles 80–200 nm in size are illustrated in Figs. 4–8. The particle combustion is completely equilibrium in terms of both temperature and velocity; it is characterized by a higher activation energy of the reduced Arrhenius kinetics taken into account in the model [14] in accordance with the experimental data [13, 19]. As was shown in [14], the scale of oscillations of the reaction zone length for overdriven and attenuated waves is appreciably greater than that in the case of detonation of micron-sized particles, which is responsible for the differences in the cellular detonation patterns. Looking at the footprints of the triple points, one can see that they are even more distinct than those in suspensions of microparticles. A comparison of Figs. 2 and 3 with Figs. 6 and 7 shows that the triple point trajectories are close to straight lines in the transitional regime of combustion; in the kinetic regime, these trajectories are close to arcs, which is typical for cellular detonation in gases.

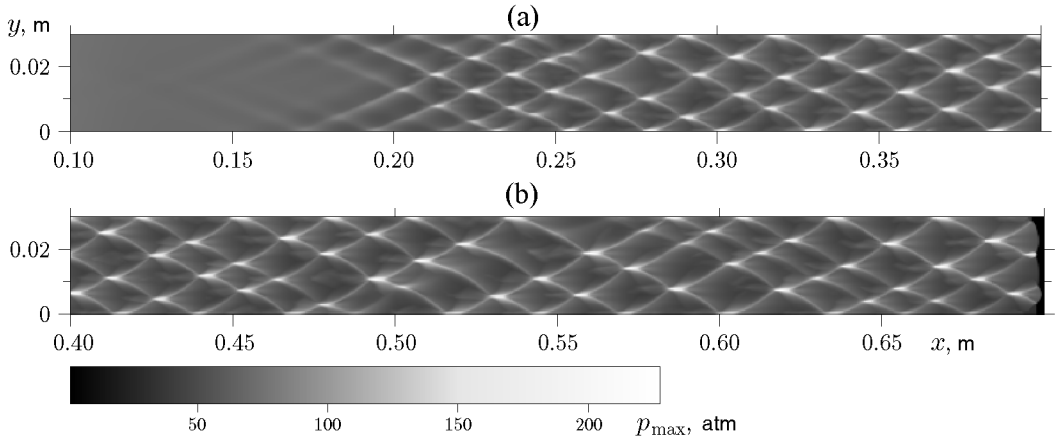

Fig. 3. Cellular detonation in a submicron suspension: the particle size is 600 nm, the channel width is 3 cm, and $\xi_0 = 0.55$.

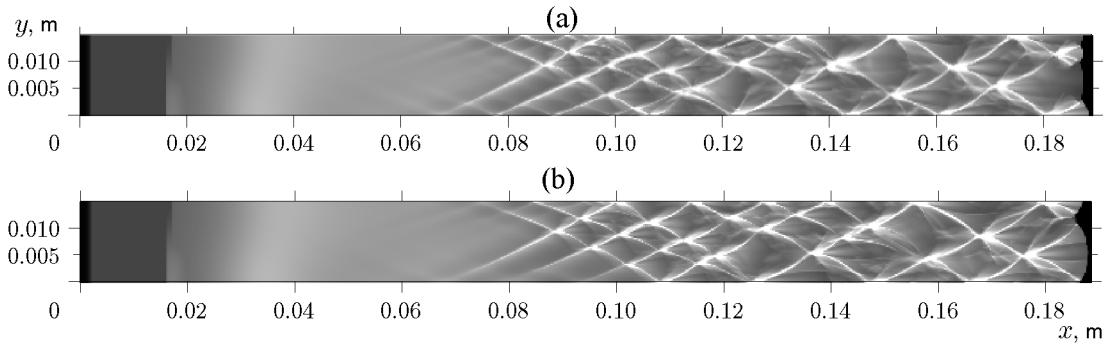

Fig. 4. Formation of cellular detonation in nano-sized suspensions in a channel 1.5 cm wide: the particle sizes are 80 (a) and 100 nm (b).

During cellular detonation development, a certain number of transverse waves is initially formed from small perturbations; the distance between these wave is predicted by the acoustic theory [11, 20]. In suspensions of microparticles, propagation and enhancement of transverse waves leads only to minor changes in the cell size [11]. In suspensions of nanoparticles, significant rearrangement of the transverse waves is observed, and the cell size becomes noticeably greater, which is observed both in narrow channels (Figs. 1, 4, and 5) and in sufficiently wide channels (Figs. 6 and 7). For example, in all fragments of Fig. 1, five initially formed transverse waves transform to two transverse waves forming one asymmetric cell under the action of the channel walls. In Fig. 4, only three transverse waves are left from five to seven waves formed at the beginning, and these three transverse waves form 1.5 cells in the channel.

In wide channels, the rearrangement of transverse waves is even more clearly visible. Figures 6 and 7 show that the cell size multiply increases in the course of detonation propagation; moreover, the number of transverse waves and, correspondingly, the number of cells in the channel become different. Thus, the character of cellular detonation of suspensions of nanoparticles can be considered as weakly regular or irregular.

It should be noted that the maximum pressure in the case of the collision of the triple points is several times higher than that in the case of cellular detonation of microparticles. For example, the pressure reaches 510 atm in the nodes in Fig. 1, 570 atm in Fig. 4, and 600–700 atm in wide channels (see Figs. 6 and 7) with an increase in the cell size. This result is qualitatively consistent with the experimental observations of spin detonation in air suspensions of aluminum particles [4], where the pressure measurements revealed a significant increase in the amplitude of fluctuations in the powder with the particle size of 100 nm as compared to a similar suspension of particles with the mean size of 1.6 μm.

The instantaneous patterns of cellular detonation in a mixture of 100-nm particles are shown in Fig. 8. More distinct patterns of the SW fronts and higher peak values of parameters than those in mixtures of

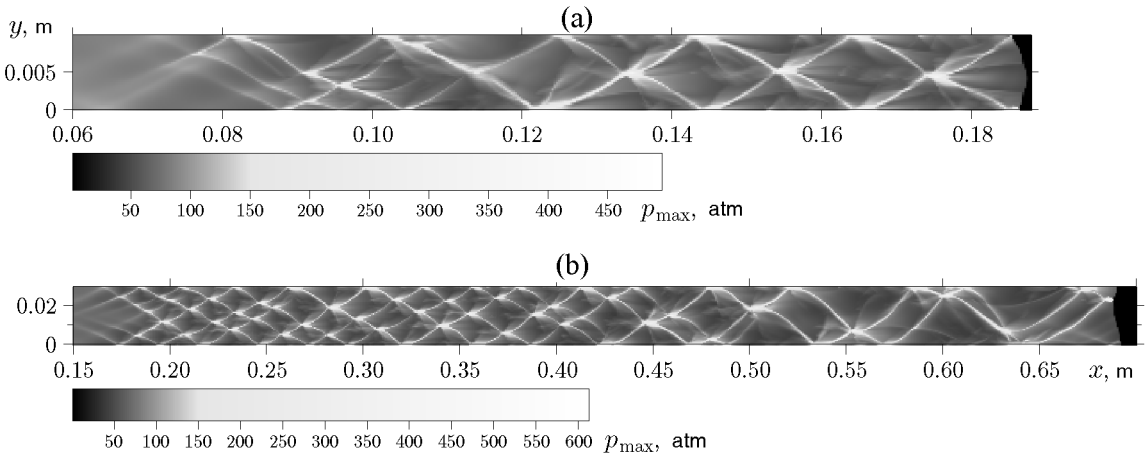

Fig. 5. Detonation propagation in narrow channels: (a) the cell size is 200 nm and the channel width is 1 cm; (b) the cell size is 150 nm, and the channel width is 3 cm.

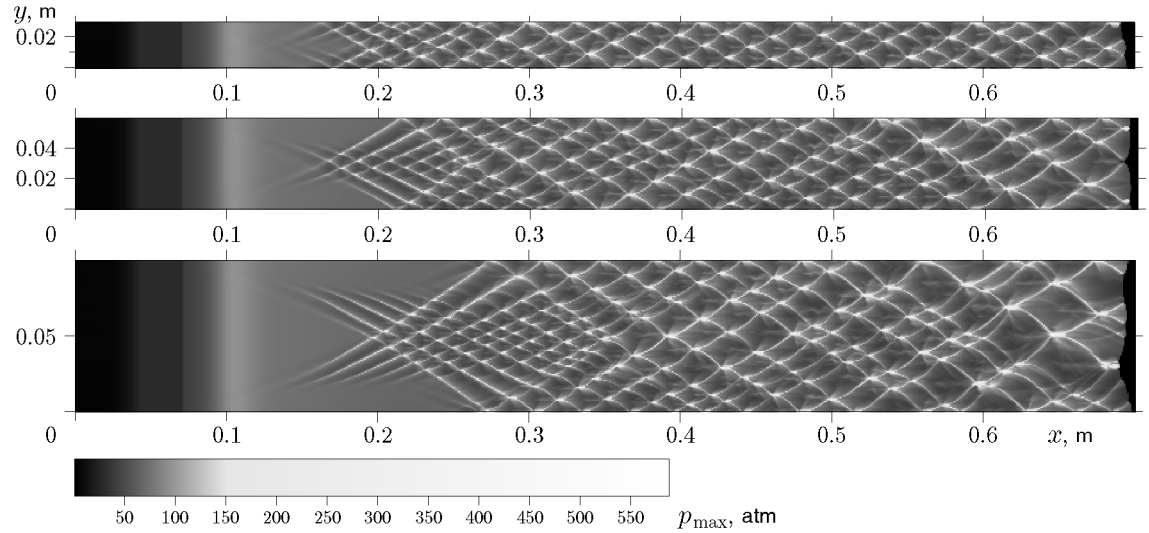

Fig. 6. Detonation propagation in a mixture of 200-nm particles in channels of different widths.

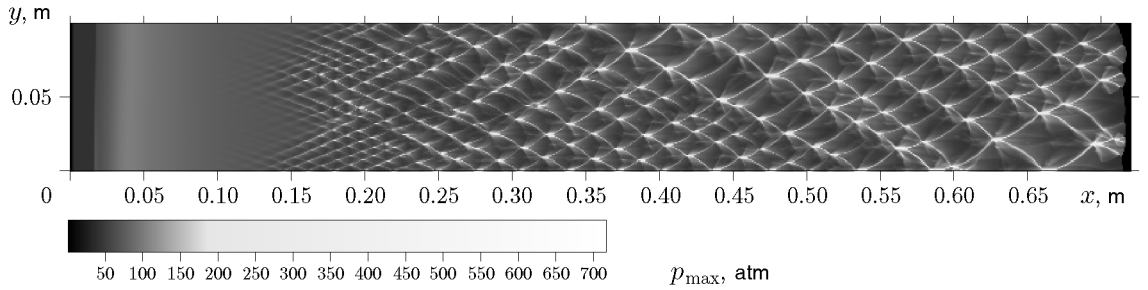

Fig. 7. Rearrangement of transverse waves during propagation of cellular detonation: the channel width is 10 cm, and the particle size is 150 nm.

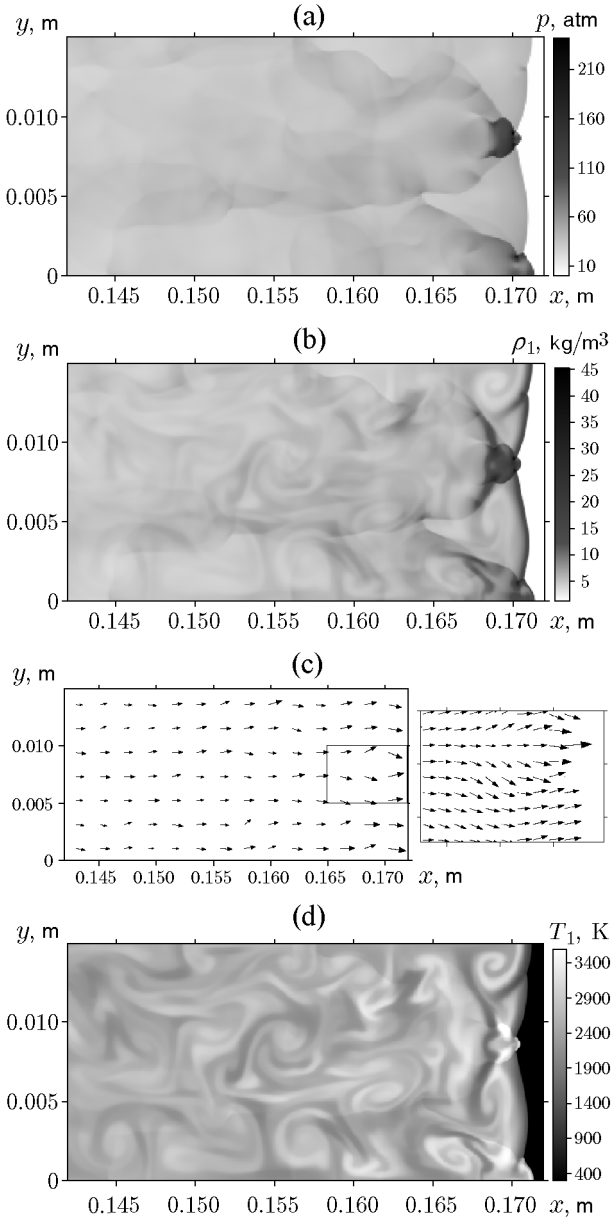

Fig. 8. Instantaneous patterns of cellular detonation: the time instant is 0.09 ms, the channel width is 1.5 cm, and the particle size is 100 nm; (a) pressure; (b) gas density; (c) velocity field; (d) temperature field.

microparticles can be also noted here. For example, the maximum value of the gas density in [11] was 14 kg/m^3, whereas the values in Fig. 8b are three times higher. The maximum pressure obtained for a monodisperse suspension of 2-μm particles in [21] was 120 atm, whereas the value in Fig. 8a for a similar configuration of overdriven and attenuated waves is 240 atm. As a whole, cellular detonation of suspensions of micro- and nanoparticles is characterized by a similar character of flow fields, pressure and density distributions, vortex structures, and temperature fields, except for more curved trajectories of the transverse wave fronts in gas suspensions of nanoparticles and the above-noted increase in the amplitude of fluctuations of hydrodynamic parameters.

CONCLUSIONS

Cellular detonation in monodisperse suspensions of submicron and nano-sized aluminum particles with a stoichiometric composition in oxygen is studied by methods of numerical simulation of two-dimensional flows within the framework of mechanics of heterogeneous media.

The processes of velocity and thermal relaxation of the gas medium with nanoparticles are described with allowance for the transition from the continuum to free-molecular flow regime around the particles. The description of combustion of aluminum nanoparticles is based on the semi-empirical model of reduced kinetics developed earlier with the use of a large number of experimental data. The model takes into account the transition from the diffusion-limited to kinetic regime of particle combustion with the power-law index of 0.3 in the dependence of the characteristic burning time on the particle diameter and the increase in the activation energy with particle size reduction.

The problem formulation corresponds to shock wave initiation of detonation in a cloud of particles in a plane channel with the development of transverse waves from small perturbations.

A specific property of cellular detonation of nanodisperse suspensions is essential rearrangement of transverse waves in the course of development of perturbations, which is accompanied by a decrease in the number of transverse waves and an increase in the cell size and peak values of the detonation parameters.

In the case of developed cellular detonation of nanodisperse suspensions, the trajectories of the transverse wave fronts are more curved, as well as the trajectories of the triple points in the peak pressure history. Based on the instantaneous flow fields, the patterns of cellular detonation of suspensions of micro- and nanoparticles are qualitatively similar in terms of pressure fields, density fields, vortex structures, and temperature distributions.

As the particle size decreases to the submicron and nano-sized range, the amplitude of fluctuations of hydrodynamic parameters, in particular, the peak pressure of cellular detonation increases, which is consistent

with the experimental data [4]. The detonation cell becomes significantly greater, and the regular character of cellular structures in the case of micron and submicron particles transforms to an irregular pattern for particles 80–200 nm in size. These specific features can be attributed to the increase in the activation energy of reduced kinetics after the transition to the kinetic regime of aluminum combustion.

This study was carried out within the framework of the Program of Fundamental Scientific Research of the State Academies of Sciences in 2013–2020 (Project No. AAAA-A17-117030610139-4).

REFERENCES

1. W. A. Strauss, "Investigation of the Detonation of Aluminum Powder–Oxygen Mixtures," AIAA J. **6** (12), 1753–1761 (1968).
2. A. J. Tulis and J. R. Selman, "Detonation Tube Studies of Aluminum Particles Dispersed in Air, in *Proc. of the 19th Int. Symp. on Combustion* (Combustion Inst., Pittsburgh, 1982), pp. 655–663.
3. W. Ingignoli, B. Veyssiere, and B. A. Khasainov, "Study of Detonation Initiation in Unconfined Aluminum Dust Clouds," *Gaseous and Heterogeneous Detonations, Science to Applications*, Ed. by G. Roy et al. (ENAS Publ., 1999), pp. 337–350.
4. F. Zhang, S. B. Murray, and R. B. Gerrard, "Aluminum Particle–Air Detonation at Elevated Pressures," Shock Waves **15**, 313–324 (2006).
5. A. V. Fedorov, "Structure of the Heterogeneous Detonation of Aluminum Particles Dispersed in Oxygen," Fiz. Goreniya Vzryva **28** (3), 72–83 (1992) [Combust., Expl., Shock Waves **28** (3), 277–286 (1992)].
6. A. A. Borisov, B. A. Khasainov, B. Veyssiere, et al., "On Detonation of Aluminum Suspensions in Air and Oxygen," Khim. Fiz. **10** (2), 250–272 (1991).
7. B. Veyssiere and B. A. Khasainov, "Model for Steady, Plane, Double-Front Detonations (DFD) in Gaseous Explosive Mixtures with Aluminum Particles in Suspension," Combust. Flame **85** (1, 2), 241–253 (1991).
8. A. V. Fedorov, T. A. Khmel, and V. M. Fomin, "Non-Equilibrium Model of Steady Detonations in Aluminum Particles–Oxygen Suspensions," Shock Waves **9** (5), 313–318 (1999).
9. F. Zhang, K. Gerrard, and R. C. Ripley, "Reaction Mechanism of Aluminum-Particle–Air Detonation," J. Propul. Power **25**, 845–858 (2009).
10. K. Benkiewicz and A. K. Hayashi, "Two-Dimensional Numerical Simulations of Multi-Headed Detonations in Oxygen–Aluminum Mixtures Using an Adaptive Mesh Refinement," Shock Waves **13**, 385–402 (2003).
11. A. V. Fedorov and T. A. Khmel', "Numerical Simulation of Formation of Cellular Heterogeneous Detonation of Aluminum Particles in Oxygen," Fiz. Goreniya Vzryva **41** (4), 84–98 (2005) [Combust., Expl., Shock Waves **41** (4), 435–448 (2005)].
12. A. Briand, B. Veyssiere, and B. A. Khasainov, "Modelling of Detonation Cellular Structure in Aluminum Suspensions," Shock Waves **20**, 521–529 (2010).
13. D. S. Sundaram, V. Yang, and V. E. Zarko, "Combustion of Nano Aluminum Particles (Review)," Fiz. Goreniya Vzryva **51** (2), 37–63 (2015) [Combust., Expl., Shock Waves **51** (2), 173–196 (2015)].
14. T. A. Khmel and A. V. Fedorov, "Modeling of Plane Detonation Waves in a Gas Suspension of Aluminum Nanoparticles," Fiz. Goreniya Vzryva **54** (2), 71–81 (2018) [Combust., Expl., Shock Waves **54** (2), 189–199 (2018)].
15. A. V. Fedorov and T. A. Khmel', "Characteristics and Criteria of Ignition of Suspensions of Aluminum Particles in Detonation Processes," Fiz. Goreniya Vzryva **48** (2), 76–88 (2012) [Combust., Expl., Shock Waves **48** (2), 191–202 (2012)].
16. A. V. Fedorov, T. A. Khmel', and S. A. Lavruk, "Exit of a Heterogeneous Detonation Wave into a Channel with Linear Expansion. II. Critical Propagation Condition," Fiz. Goreniya Vzryva **54** (1), 81–90 (2018) [Combust., Expl., Shock Waves **54** (1), 72–81 (2018)].
17. A. V. Fedorov and T. A. Khmel, "Numerical Technologies in Investigations of Heterogeneous Detonation of Gas Suspensions," Mat. Model. **18** (8), 49–63 (2006).
18. B. Veyssiere, B. A. Khasainov, and A. Briand, "Investigation of Detonation Initiation in Aluminum Suspensions," Shock Waves **18**, 307–315 (2008).
19. T. Bazyn, H. Krier, and N. Glumac, "Combustion of Nanoaluminum at Elevated Pressure and Temperature behind Reflected Shock Waves," Combust. Flame **145**, 703–713 (2006).
20. H. O. Barthel, "Predicted Spacings in Hydrogen–Oxygen–Argon Detonations," Phys. Fluids **17** (8), 1547–1553 (1974).
21. A. V. Fedorov and T. A. Khmel', "Formation and Degeneration of Cellular Detonation in Bidisperse Gas Suspensions of Aluminum Particles," Fiz. Goreniya Vzryva **44** (3), 109–120 (2008) [Combust., Expl., Shock Waves **44** (3), 343–353 (2008)].